ELSEVIER

CrossMark

Available online at www.sciencedirect.com

ScienceDirect

Energy Procedia 63 (2014) 6800 – 6814

Energy Procedia

GHGT-12

Sustainable Hydrogen Production from Biogas Using Sorption-Enhanced Reforming

Julien Meyer[a] *, Johann Mastin[a], Cristina Sanz Pinilla[a]

[a]*Institute for Energy Technology, P.O. Box 40, NO-2027 Kjeller, Norway*

Abstract

The interest in the use of upgraded biogas for the introduction of renewable hydrogen through reforming technologies is steadily increasing. Renewable hydrogen as fuel for power production or transportation is one major application area. The novel sorption-enhanced reforming (SER) technology including CO_2 capture has the potential to introduce renewable hydrogen to the marked and at the same time provide bio-CO_2 that can be used to produce biomethane through the Sabatier process. This paper presents the work carried out to design and build a small SER prototype using a dual bubbling fluidized bed reactor system. Reactor modeling and advanced computational fluid dynamics have been used to dimension and evaluate the performance of the installation. Preliminary laboratory tests have allowed validating the design and the system specifications. Finally, initial batch tests run on the installation have proved the feasibility of operating the process. The next phase of this work will involve the coupling of the solids circulation loop to operate the system continuously.

© 2014 The Authors. Published by Elsevier Ltd. This is an open access article under the CC BY-NC-ND license
(http://creativecommons.org/licenses/by-nc-nd/3.0/).

Peer-review under responsibility of the Organizing Committee of GHGT-12

Keywords: Hydrogen ; Biogas ; Sorption-Enhanced Reforming ; Fluidized Bed Reactor

---

1. Introduction

Hydrogen is widely considered as a sustainable CO_2-free energy carrier for stationary and mobile applications, such as decentralized power production, and for the transport sector. Its use as transportation fuel in Fuel Cell Hydrogen Vehicles (FCHV) has been successfully demonstrated in several international projects both in Europe, North America and Asia [1, 2], and several car manufacturers plan the introduction of FCHVs on the market by 2015-2017. For decentralized small and medium scale hydrogen production, two main routes have been developed:

---

* Corresponding author. Tel.: +47-46-61-43-89.
E-mail address: julien.meyer@ife.no

1876-6102 © 2014 The Authors. Published by Elsevier Ltd. This is an open access article under the CC BY-NC-ND license
(http://creativecommons.org/licenses/by-nc-nd/3.0/).

Peer-review under responsibility of the Organizing Committee of GHGT-12
doi:10.1016/j.egypro.2014.11.714

water electrolysis and reforming of gaseous carbonaceous fuels. However, to use hydrogen as a CO_2-free energy carrier, electrolysis is depending on green electricity supply and reforming requires either the use of a CO_2 capture unit (with transport and storage facilities) and/or the use of biomethane produced from biogas or biomass.

There are three main routes to produce biogas: through anaerobic digestion, through gasification and methanation, and through the reduction of bio-CO_2 with renewable hydrogen via the Sabatier process [3]. The latter is seen as a third generation biofuel and is now considered as an interesting option to increase the production of biofuels on the market. However, this production route requires the use of bio-CO_2. Biogas produced in anaerobic digesters from sewage sludge, food waste or animal manures is now widely available worldwide in different amounts. It has so far mainly been used for power production and as transportation fuel after an upgrading step, but has recently been considered as a viable alternative to introduce significant amounts of renewable hydrogen on the market.

Conventional Steam Methane Reforming (SMR) is currently the preferred technology to produce hydrogen from biogas via biomethane. At small and medium scale, this process involves three main steps: reforming, water-gas shift and hydrogen purification where CO_2 is removed from the process along with methane, carbon monoxide and nitrogen impurities. If CO_2 is to be separated in this production route to produce valuable bio-CO_2, a costly extra removal step has to be added.

Since the late nineties, hydrogen production using Sorption-Enhanced Reforming (SER) has been investigated by several research groups and is now considered as an emerging promising reforming technology. This technology involves only two main process steps and CO_2 capture as an integrated part of the process. Therefore, it has the potential to both reduce the production cost of renewable hydrogen and to supply valuable bio-CO_2 for the production of additional biomethane via the Sabatier process. Moreover, since CO_2 capture is an integrated part of the process, the technology has the possibility to avoid the costly biogas upgrading step. Therefore, the novel SER reforming technology can, on a medium term perspective, contribute to a more efficient and profitable production of renewable hydrogen with integrated CO_2 capture.

1.1. Aim and scope of the study

In order to bring the SER technology forward to up-scaling and commercialisation, knowledge regarding stable operation of a reactor system suited to the SER process in steady state continuous operating conditions is needed. Production of reliable experimental data at small pilot level also represents an important step towards design of medium to large scale SER demonstration plants running on biomethane.

This paper will present the work carried out to design and build a small scale SER prototype using a Dual Bubbling Fluidized Bed (DBFB) reactor system installed at the HyNor Lillestrøm renewable hydrogen technology test centre, 25 km east of Oslo, Norway [4]. Results from preliminary laboratory tests and from the first tests run on the prototype will also be presented in the paper.

2. Sorption-enhanced reforming (SER)

Sorption Enhanced Reforming (SER) is an emerging technology for hydrogen production with integrated CO_2 capture which combines the reforming and water gas shift reactions with a calcium looping cycle for CO_2 capture based on a high temperature carbonation-calcination cycle. The process involves the use of a high temperature CaO-based CO_2 solid sorbent together with a reforming catalyst, usually nickel based [5]. In the process, reforming, water gas shift (WGS) and CO_2 capture (carbonation) occur simultaneously. The process takes advantage of the Le Chatelier principle which, due to the simultaneous in-situ CO_2 sorption in the sorbent, results in a shift of the thermodynamic equilibrium towards production of hydrogen, thereby enhancing the hydrogen yield. The combination of these three chemical reactions results also in an almost auto-thermal overall reaction, with a broad operation temperature window. The process has to be regenerative, and to release the captured CO_2, the SER looping cycle requires a second reaction vessel where the CO_2 sorbent is regenerated in a calcination reaction by increasing the temperature beyond the decomposition temperature of $CaCO_3$. The chemical reactions (1) to (5) involved in the process are as follows:

$$CH_4(g) + H_2O(g) \rightarrow 3H_2(g) + CO(g) \quad (1)$$

$$CO(g) + H_2O(g) \rightarrow H_2(g) + CO_2(g) \quad (2)$$

$$CaO + CO_2(g) \rightarrow CaCO_3 \quad (3)$$

$$CH_4(g) + 2H_2O(g) + CaO \rightarrow 4H_2(g) + CaCO_3 \quad (4)$$

$$CaCO_3 \rightarrow CaO + CO_2(g) \quad (5)$$

The main advantages of the SER process compared to conventional SMR are that fewer reaction vessels are required, that there is no need for shift catalysts and CO_2 solvents, that a higher hydrogen yield (95 to 99 mole%, dry basis) can be reached in one single step, and that a general process simplification and intensification leads to higher efficiency. In addition, near to pure CO_2 is obtained by regenerating the CO_2-sorbent using high temperature heat.

Sorption-enhanced reforming has been successfully demonstrated at laboratory scale with natural CaO-based sorbents (dolomite and calcite) both in a fixed bed system [6] and in a fluidized bed system [7]. However, these natural sorbents show limitations of their multi-cycle ability as their sorption capacity and reaction kinetics decrease with the number of cycles, mainly due to sintering and pore closure effects [8]. In recent years, several research groups have therefore been working on the development of synthetic CaO-based solid sorbents showing better performances then natural sorbents [9]. This research is now focused on maximizing sorption capacity and multi-cycling ability as well as minimizing the production costs.

In order to model the SER process, kinetics models are required. Correlations for the reaction rates are available in the literature considering a two-particle system (sorbent and catalyst). Such models have been used in numerical analyses by Lindborg et al. [10]. Considering the particle models, the structural changes in the spherical grains due to the product layer have been considered in various ways [11]. Three different approaches based on the random pore model, the shrinking unreacted core model and the grain model are reported for carbonation reaction of CaO with CO_2.

Extensive work has also been carried out in the field of reactor and process modelling adapted to the SER process for H_2-production [12, 13]. Several modelling concepts are available for modelling fluidized beds, but the two-fluid model concepts are normally preferred due to the feasible computational efforts required. Wang et al. [14] have simulated the performance of SER in fluidized bed reactors operated in different flow regimes.

The SER process can be operated in a batch mode using several fixed bed reactors operating in a sequence, or in a continuous mode by circulating the solids between two reactors operating in steady state. The latter can be accomplished by using two coupled fluidized bed reactors where different configurations are possible.

Contrary to the SER reaction, the sorbent regeneration step of the process requires heat. This heat can be supplied directly using an oxy-fuel combustion system, or indirectly using an integrated high temperature heat exchanger in the regenerator. Two examples of the reactor configurations that can be used in the process are illustrated in Fig. 1.

Running the process in a batch mode, the SER reaction can be pressurized up to pressures usually used in the standard reforming process (15-20 bar) to reduce the size of the reformer reactor. On the other hand, increasing the pressure of the regeneration step of the process will require a higher calcination temperature, increase the amount of heat to be supplied, and is therefore not advantageous. Pressurization of the process up to a few bars (3 bar) is also possible if the process is run continuously with coupled fluidized bed reactors, the limiting factor being the calcination temperature.

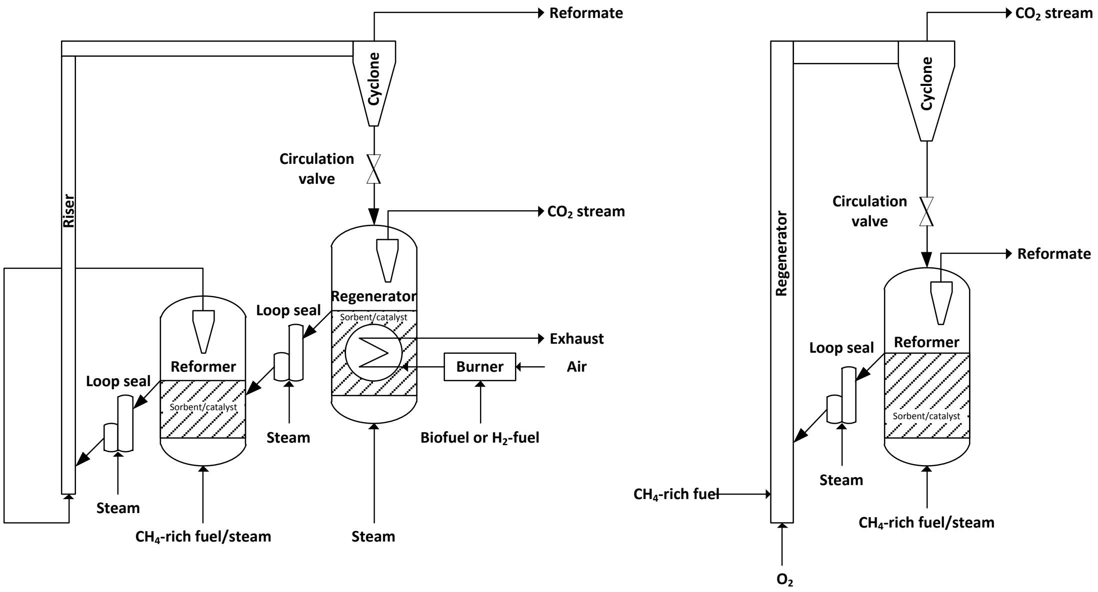

Dual Bubbling Fluidized Bed (DBFB) configuration with indirect heat exchange

Circulating Fluidized Bed (CFB) configuration with oxy-fuel direct heat exchange

Fig. 1. Two examples of the reactor configurations that can be used for the SER process.

3. Design of the Dual Bubbling Fluidized Bed (DBFB) reactor system

3.1. Reactor configuration and specification of the SER prototype

The continuous nature of the SER process makes the use of a fluidized bed reactor technology with circulation of solids a natural choice to run the process in an efficient manner. Fluidized bed reactors show also advantageous properties for running the process, such as good temperature homogeneity, excellent heat transfer, and the possibility to add or purge solids under operation. As shown in Fig. 1, two different reactor configurations are possible. The Dual Bubbling Fluidized Bed configuration (DBFB) with a submerged heat exchanger in the regenerator has been chosen for the prototype, mainly to avoid the oxidation-reduction cycle of the commercial nickel based reforming catalyst which could alter its stability and performance. A hydrogen production capacity of about 10 Nm^3/h has been considered as a suitable scale for demonstration purpose. The DBFB prototype is operated at near atmosphere pressure. The sorbent used in the DBFB reactor system is a calcined Arctic dolomite (CaOMgO) and the catalyst is a commercial $Ni/Mg_2Al_2O_4$ reforming catalyst containing 12 to 15 wt.% Ni. Fig. 2 shows a sketch of the SER DBFB prototype.

3.2. Reactor modeling of the DBFB system and dimensioning

A previously developed two-phase hydrodynamic fluidized bed reactor model for the circulating DBFB system has been used as a tool to dimension the system and to evaluate its performance [12]. In this model, referred to as the Orcutt model [15], the fluidized bed consists of two phases, a bubble and a dense phase called emulsion. Each phase is described by separate equations, including a term describing interfacial mass transfer. The two-phase theory states that all gas in excess of that necessary to fluidize the bed passes through the bed as bubbles. The gas flow in the bubbles is modelled as plug flow and the gas in the dense phase is considered perfectly mixed. Mass transfer between the two phases is represented by an interphase mass transfer coefficient. Reaction kinetics, thermodynamics and heat and mass balances are taken into account in the model. The carbonation kinetics model uses a shrinking unreacted-core model and is described by Johnsen [16]. The rate expressions for the catalytic SMR reaction are those proposed by Xu and Froment [17] who used a $Ni/MgAl_2O_4$ catalyst.

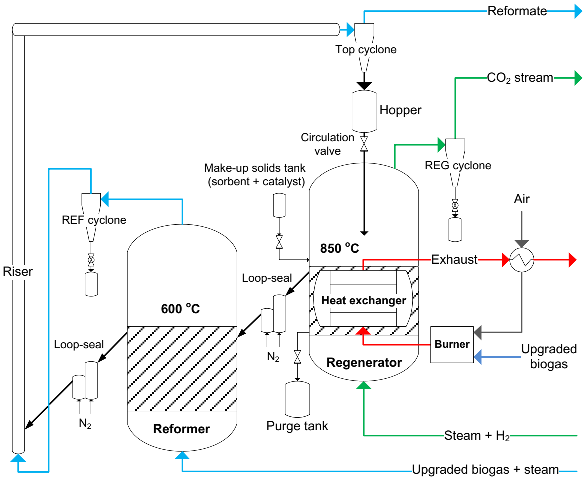

Fig. 2. Sketch of the SER DBFB prototype.

The main inputs to the circulation reactor model are:

- Hydrogen production capacity
- Steam to carbon molar ratio
- Reformer and regenerator inner diameters
- Reformer and regenerator temperatures
- Sorbent to catalyst mass ratio
- Solids properties (particle size, density, heat capacity)
- Sorbent conversion

The regenerator's dimensions and performance have to take into account the submerged high temperature heat exchanger, and they have been optimized separately. Section 3.4 describes this part.

Solids data are given in Table 1. The operating conditions and the main dimensions are given in Table 2 and 3.

3.3. Description of the DBFB system

The SER DBFB system is operated with an upgraded biogas following the Swedish standard for biogas as vehicle fuel SS155438.

The upgraded biogas is first mixed with process steam, and the mixture is pre-heated to 200 °C before being fed to the reformer. The reformer is operating at 600 °C, and additional heat is supplied by the solids returned from the regenerator, which is operated at 850 °C. In the reformer, hydrogen is produced and the CO_2 is captured simultaneously at high temperature. The product gas (reformate) from the reformer mainly consists of hydrogen and steam, with only minor quantities of CO, CO_2, N_2 and unconverted CH_4. The reformate passes through an external cyclone to remove entrained solids from the reformer. The solids from the reformer are transported to the regenerator in a transport riser (0.067 m inner diameter, 4.5 m high), using the reformate gas as transport medium. Solids and reformate gas pass through a high efficiency cyclone to separate the solids and the transport gas. The solids first fall in a hopper and are then introduced in the regenerator at an optimum circulation rate thanks to a slide valve. The CO_2-containing sorbent is heated in the regenerator and CO_2 is released. The heat required in the regeneration step is supplied indirectly via a submerged U-tube high temperature heat exchanger in the regenerator. This heat is supplied by the exhaust gas of a biogas-fired external catalytic burner. Steam with 2 vol% hydrogen is used as fluidization medium and is supplied to the regenerator at about 800 °C. The CO_2 stream from the regenerator passes through a cyclone to remove entrained particles before being heat exchanged with the regenerator feed and cooled. The reformate gas is further cleaned in a hot filtration unit operated at 350 °C before being heat exchanged with the reformer steam feed and cooled. Non-mechanical valves, called loop-seals, are used to ensure that there is no mixing of gases between the reactors and to allow smooth solids transfer. Pictures of the installation are shown in Fig. 3.

Table 1. Solids data.

Average particle size of solids mixture	160.10^{-6} m
Calcined sorbent particle density	1600 kg/m^3
Catalyst particle density	2200 kg/m^3
Solids mixture mass heat capacity	1032 J/kg.K
Sorbent CaO content (calcined)	59.8 wt.%

Table 2. General operating conditions of the DBFB system.

Steam to carbon molar ratio	4
Sorbent to catalyst mass ratio	2.8
Sorbent molar conversion	0.22
Solids circulation rate	76 kg/h
Required heat supply to regenerator	12.5 kW

Table 3. Operating conditions and main reactor dimensions.

	Reformer	Regenerator
Reactor temperature	600 °C	850 °C
Reactor bed diameter	0.2545 m	0.45 m
Fluidization velocity	0.29 m/s	0.10 m/s
Solids inventory (sorbent + catalyst)	21 kg	78 kg
Expanded bed height	0.59 m	0.73 m
Freeboard inner diameter	0.348 m	0.636 m
Freeboard height	1.20 m	0.85 m

To simplify the process, and although there is enough heat available, the process steam feeds of the two reactors are produced by a 36 kW electrically heated steam generator delivering saturated steam at a pressure up to 3 bara.

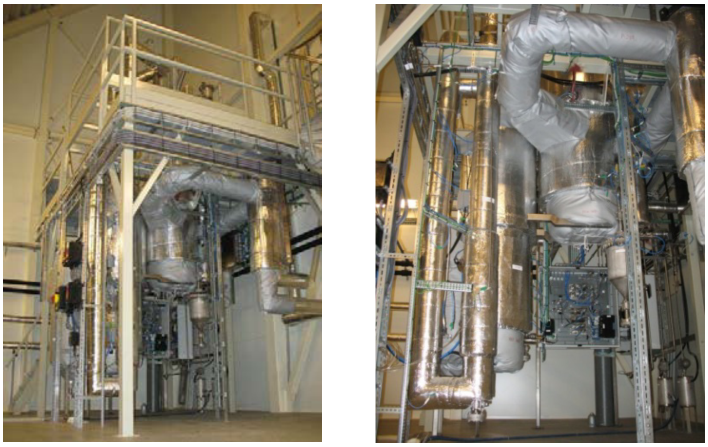

Fig. 3. Pictures of the SER DBFB prototype.

3.4. Design of the high temperature heat exchanger submerged in the regenerator

The chosen design of the high temperature heat exchanger (HT-HX) in the regenerator uses a vertical U-tubes bundle. The tubes are bent in one single part and are welded on the inlet and outlet of the heat exchanger housing. They can expand freely downwards but they apply a radial stress on both sides of the heat exchanger housing. Their U-shape gives them flexibility. Two manifolds are welded on the inlet and outlet to first distribute and then collect the hot heat exchange medium (hot exhaust gas from the burner). Inconel 601 is chosen as tube material due to its good mechanical strength and its outstanding resistance to oxidation at high temperature. The heat exchanger housing, where the tubes and the manifolds are welded on, is in Incoloy 800HT.

The regenerator is dimensioned to allow sufficient space for the insertion of the required heating surface for the calcination reaction. The solids inventory and the fluidization velocity are adjusted so that the heat exchanger is totally immersed in the expanded bed volume. The gap between adjacent surfaces must normally exceed 30 to 50 mean particle diameters in order to allow the particles to circulate freely through the open spaces between the fixed surfaces. This distance has been chosen equal to 0.015 m. The geometry data of the heat exchanger, together with the particle bed and the process conditions in the regenerator, are given in Table 4.

Table 4. Geometry data of the high temperature heat exchanger of the regenerator.

HT-HX housing inner diameter	0.45 m
Number of U-tubes	35
U-tube outer diameter	0.02134 m
U-tube wall thickness	0.00277 m
Total immersed U-tube length	46.8 m
Average single U-tube length	1.34 m
Total immersed tube area	3.14 m^2
HT-HX height	0.514 m
Expanded bed height	0.73 m

3.5. Heat transfer calculations and CFD analysis of the heat exchanger tubes

For dense bubbling beds, it is recognized that mechanisms contributing to heat transfer at submerged surfaces include gaseous convection during times of bubble contact, particle conduction/convection during times of particle contact, and radiation in the case of high temperature operation [18]. The effective heat transfer coefficient is often represented by the sum of the convective term, h_c, and the radiative term, h_r.

$$h = h_c + h_r \tag{6}$$

Several approaches have been proposed for the estimation of h_c. All have their advantages and disadvantages, and all involve some degree of empiricism. For this study, the convective heat transfer coefficient is estimated by using the approach of Morelus et al. [19] which considers combined gaseous and particle convection for nearly spherical particles. Radiative heat transfer needs to be taken into account at the high temperature employed in the regenerator as the radiant contribution to overall heat transfer increases with temperature. At 800 °C, this contribution is reported to be greater than 35% of the total heat flux in a bubbling bed [20]. The simplest approach to calculate h_r, is to use the Stefan-Boltzman equation for radiant exchange between opaque and grey bodies. The equations that summarize the calculation of the convective and radiative heat transfer coefficients are shown in Appendix A.

Taking into account a solid circulation rate of 76 kg/h, a sorbent molar conversion of 0.22, and an overall fluidization velocity of 0.10 m/s, a gas composition in the regenerator containing 77.4 vol% steam, 21 vol% CO_2 and 1.6 vol% H_2 has been estimated. Gas density, viscosity and thermal conductivity for this composition have been obtained from the Aspen HYSYS data base (Aspen Technology Inc.). Heat capacities of pure solid compounds have been used to calculate the heat capacity of the sorbent-catalyst mixture in the regenerator.

To calculate the radiative heat transfer coefficient, emissivities of both the bed and the tubes are required. With reference to Ozkaynak et al. [20], an approximate bed emissivity of 0.9 has been chosen. A hemispherical emissivity of 0.805 for the Inconel material has been selected (Special Metals; Technical Bulletin).

The key parameters for the calculation of the heat transfer coefficient of the HT-HX are summarized in Table 5.

Table 5. Key parameters for calculation of the heat transfer coefficient of the HT-HX.

Gas density	0.2521 kg/m^3
Gas viscosity	3.71 10^{-5} Pa.s
Gas thermal conductivity	0.09168 W/m.K
Gas heat capacity	1941 J/kg.K
Sorbent-catalyst mixture density	1724 kg/m^3
Sorbent-catalyst mixture heat capacity	1032 J/kg.K
Bed voidage at minimum fluidization	0.5
Bed emissivity	0.9
Tube hemispherical emissivity	0.805
Total immersed tube area	3.14 m^2
Minimum required heat to be transferred	12.5 kW

The convective heat transfer coefficient $h_{c,tube\text{-}bed}$ between the heat exchanger tubes and the gas/particle bed is first calculated for a gas/particle bed temperature of 850 °C and for the operating fluidization regime. Then the outer tube temperature is calculated and adjusted to match the total immersed surface area of the heat exchanger through an iterative calculation. The results are summarized in Table 6.

Table 6. Heat transfer coefficients of the HT-HX and outer tube temperature.

Convective heat transfer coefficient (tube-bed)	528 W/m^2.K
Radiative heat transfer coefficient (tube-bed)	239 W/m^2.K
Overall heat transfer coefficient (tube-bed)	767 W/m^2.K
Calculated required outer tube temperature	855 °C

The heat transfer coefficient from the burner hot exhaust gas and the pressure drop through the HT-HX are of special interest to match the heat transfer requirement from the exhaust gas to the bed. Therefore, a Computational Fluid Dynamics (CFD) study has been carried out to quantify these two parameters.

The simulations have been run for a burner exhaust gas temperature of 1050 °C and with compressible fluid. Different inlet velocities are specified in the range of 10 to 50 m/s. The inlet gas flow has been simulated with uniform temperature and uniform velocity. The heat transfer from the burner exhaust gas to the inner tube wall is the limiting factor, thus the heat transfer through the tube wall has been neglected. An average tube length of 1.34 m has been used and the tube is assumed to be fully submerged in the fluidized bed. The inner tube temperature has been set to 857 °C and the inner tube wall is modelled as a heat sink with infinite size and constant temperature. The simulation parameters are summarized in Table 7.

Table 7. Simulation parameters of the CFD analysis of the HT-HX.

Burner exhaust gas temperature (inlet gas)	1050 °C
Inner tube temperature	857 °C
Outlet pressure	1.12 bara
Inlet gas viscosity	6.085 10^{-5} Pa.s
Inlet gas heat capacity	1225 J/kg.K
Inlet gas thermal conductivity	0.08516 W/m.K

A design margin has been taken into account in the simulation and the target required power to be transferred has been set to 15 kW to compensate for heat losses. The heat transfer and the pressure drop for different inlet gas velocities, as well as the outlet gas temperature profile through one tube, are shown in Fig. 4. The analysis shows that an inlet velocity of at least 38 m/s and a heat exchange medium at 1050 °C are sufficient to transfer 15 kW to the regenerator. This inlet velocity gives an acceptable pressure drop of about 900 Pa. The analysis gives a clear indication that the heat demand in the regenerator can be met with the specified geometry and burner exhaust flow. In the DBFB prototype, the solids enter the regenerator on the hottest side of the heat exchanger.

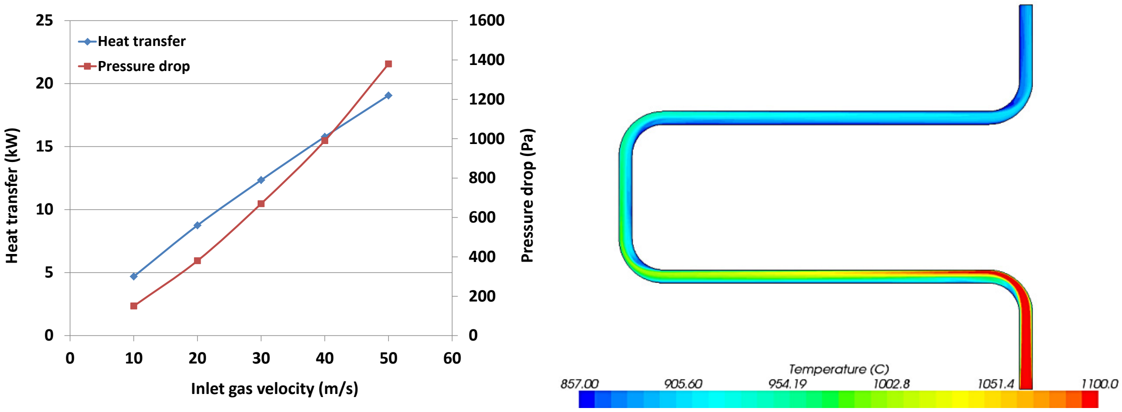

Fig. 4. Heat transfer and pressure drop as a function of gas inlet velocity in the HT-HX tubes ; Outlet gas temperature profile at the symmetry plane through one tube of the heat exchanger.

4. Experimental work

4.1. Preliminary laboratory tests

Prior to running the first tests on the DBFB prototype, separate experimental tests concerning the pre-treatment of the dolomite sorbent and the protection of the reforming catalyst against oxidation have been run in a 0.2 m inner diameter batch fluidized bed reactor (electrically heated).

Natural sorbents, such as dolomite, are widely available and cheap and are therefore often chosen at first. However, their original mechanical stability is altered by the chemical carbonation-calcination cycling and by attrition. The Arctic dolomite used in the SER process contains also traces of sulphur in the form of metal sulphates. These sulphur compounds decompose during the SER reaction and poison the nickel catalyst by forming nickel sulphide.

A thermal pre-treatment method has been developed and tested to remove the initial formation of fines during the first calcination, to improve the mechanical properties of the sorbent, and to remove the sulphur naturally present in the sorbent.

The raw dolomite has been calcined first in nitrogen at 850 °C with a bubbling fluidization velocity set to 0.1 m/s. Secondly, a two-step method to remove sulphur as hydrogen sulphide gas has been applied. In the first step, a reduction of the sulphate compounds to sulphide is achieved by fluidizing the calcined sorbent with a mixture of hydrogen in nitrogen (50 vol%) at 850 °C. The second step involves the reaction of the sulphides formed with a mixture of steam in nitrogen (50 vol%), also at 850 °C, to form the corresponding oxides and H_2S gas, thus removing the sulphur content of the material. These two steps were carried out in the same batch fluidized bed reactor with a fluidisation velocity set to 0.1 m/s for a duration of 3 hours each. The corresponding equations are shown below, where *Me* represents a metal.

$$MeSO_4 + 4H_2(g) \rightarrow MeS + 4H_2O(g) \tag{7}$$

$$MeS + H_2O(g) \rightarrow MeO + H_2S(g) \tag{8}$$

The sorption capacity and the carbonation/regeneration cycling ability of the calcined sorbent after pre-treatment have been tested in a tube oven set-up. An illustration of the set-up is shown in Fig. 5. The oven has three heating zones of about 10 cm each. The third zone was heated to 850 °C for the regeneration, while the two other zones were maintained at 600 °C for carbonation. The temperature profiles in the oven are quite sharp, so cooling and heating of the samples when transferred between the zones is fast. About 300 mg of pre-treated sorbent were loaded on a refractory crucible which was moved manually inside the tube oven flushed with a controlled gas atmosphere. The sorbent was distributed in the crucible as a thin layer. To reach the sorbent conversion foreseen in the DBFB pilot, the sample was carbonated for 1 minute and 15 seconds in 15 vol% CO_2, 38 vol% steam balanced with nitrogen. After carbonation, the sample was moved to the regeneration zone where it was calcined for 2 minutes at 850 °C in 28 vol% CO_2 and 72 vol% steam. After regeneration, the sample was moved to the carbonation zone and left to cool down and equilibrate for 1 minute in nitrogen and steam before starting a new carbonation cycle. About 25 mg of pre-treated dolomite were sampled at regular intervals (cycle number 2, 5, 15, 30) to measure the sorption capacity and the sorption kinetics in a Thermo-Gravimetric Analyzer (TGA).

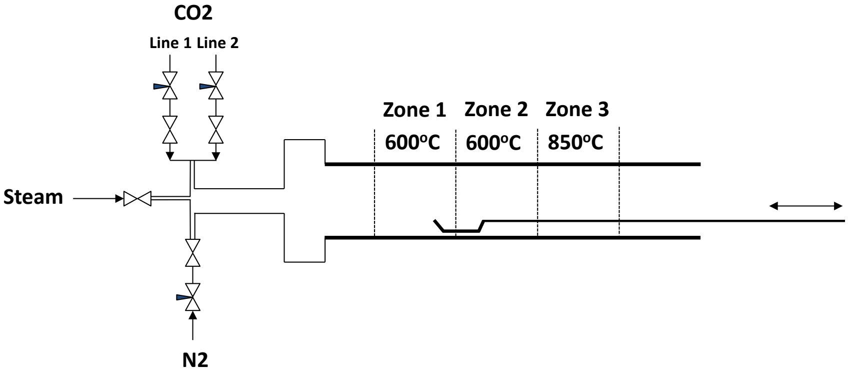

Fig. 5. Tube oven set-up.

Further, two identical SER tests were run with upgraded biogas as fuel in the batch fluidized bed reactor, with a regeneration step in between, where a small amount of hydrogen was added to the steam/nitrogen flow to protect the reforming catalyst from oxidation. The SER tests were run at 600 °C with a steam to carbon ratio of 4 and a fluidization velocity of 0.1 m/s. The sorbent to catalyst ratio was identical to the one used in the DBFB, i.e. 2.8 w/w. The regeneration was run at 850 °C in steam/nitrogen where 2 vol% hydrogen were added, and at a fluidization velocity of 0.1 m/s.

4.2. Reforming and regeneration tests on the SER DBFB prototype

The reformer reactor of the DBFB prototype has been filled with the pre-treated sorbent and reforming catalyst (sorbent to catalyst ratio of 2.8 w/w) according to the calculated solids inventory of 21 kg. As part of the pre-commissioning phase of the installation, a SER batch test with upgraded biogas as fuel has first been run in the reformer reactor at 600 °C, with a steam to carbon ratio of 4 and a fluidization velocity of 0.29 m/s. The reformer was electrically heated to maintain the operating temperature since both reactors were not coupled yet. Then, after cooling, part of the solids from the reformer have been filled in the regenerator, and a solid inventory of 65 kg was adjusted with pre-treated sorbent and catalyst in the right proportion. Further, a regeneration test has been run using first electrical heating up to 750 °C before igniting the burner and using only the burner exhaust gas as heating medium in the HT-HX. The regenerator was fluidized with nitrogen and steam with 2 vol% hydrogen added, and with a fluidization velocity of 0.1 m/s.

5. Results from the experimental work

5.1. Preliminary laboratory tests

The pre-treated dolomite sorbent has been analysed in an X-Ray diffractometer, sieved, and the particle distribution has been measured. Fig. 6 shows a diffractogram of the material mixed with the reforming catalyst. No sulphur compounds were detected. The average measured particle size of the pre-treated dolomite is 180 µm while the one of the raw dolomite is 187 µm, showing that the material shrinks a little during pre-treatment. Looking at the particle fractions for the two materials from Table 8, it can be noticed that the pre-treated sorbent contains a minor quantity of fines. However, the majority of fines that have been produced during pre-treatment have been removed by the entrainment of the fluidized bed and collected in the filter.

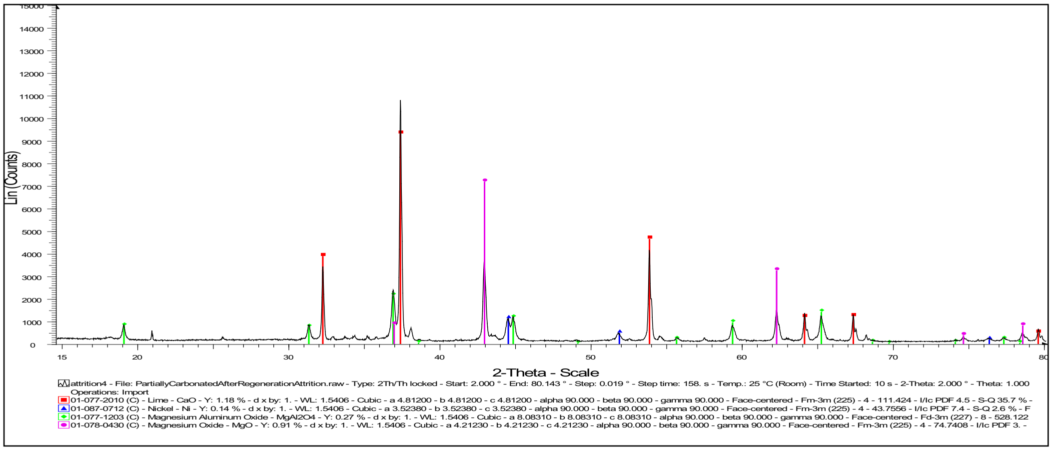

Fig. 6. XRD diffractogram of the pre-treated calcined sorbent mixed with reforming catalyst.

Table 8. Particle fractions of the raw dolomite and pre-treated dolomite.

Particle fraction, µm	Raw dolomite, wt.%	Pre-treated dolomite wt.%
200-250	32.1	34.3
150-200	65.7	58.4
100-150	2.2	5.7
75-100	0	1.3
0-75	0	0.3

The reason for studying the sorption capacity of the sorbent in the tube oven set-up is mainly that the heating and cooling times are significantly reduced compared to the cycling in a conventional Thermo-Gravimetric Analyser (TGA), thus reducing the sintering of $CaCO_3$ during heating to the regeneration temperature and preventing premature calcination. The multi-cycling in the tube oven is therefore expected to be more representative of the thermal history the sorbent will experience during operation in the DBFB. The carbonation kinetics of the 2nd, 5th, 15th and 30th cycles for cycling in the tube oven set-up are shown in Fig. 7.

The results show that from the 5th cycle, the early carbonation kinetics (i.e. during the first minute) are quite similar, indicating a stable initial uptake of CO_2 with increasing number of cycles. The sorption capacity stabilizes at around 14 g CO_2/100 g sorbent for the 30th cycle corresponding to a sorbent molar conversion of about 30%, which is higher than the 22% used in the design of the DBFB. This 22% molar conversion, corresponding to about 10 g CO_2/100 g sorbent, is achieved after around 3 minutes which is much lower than the solids residence time in the reformer, indicating that a high hydrogen yield and a high CO_2 capture rate should be achievable in the DBFB prototype.

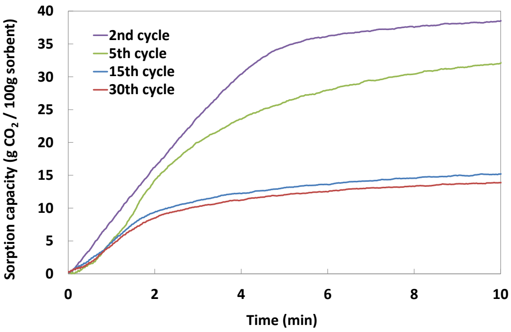

Fig. 7. Carbonation kinetics of pre-treated dolomite for cycle 2, 5, 15 and 30 for cycling in the tube oven set-up.

The results from the SER tests run with upgraded biogas as fuel in the laboratory batch fluidized bed reactor are shown in Fig. 8. A regeneration step with steam/nitrogen and 2 vol% hydrogen as fluidization gas has been run in between the SER tests. Since the hydrogen yield in both runs is quite similar (around 98 vol%), it clearly shows that no oxidation of the commercial nickel catalyst occurs during the regeneration. The use of 2 vol% hydrogen addition in the steam feed is therefore efficient to protect the reforming catalyst from oxidation-reduction cycles and should also help keeping its optimum performance in the process.

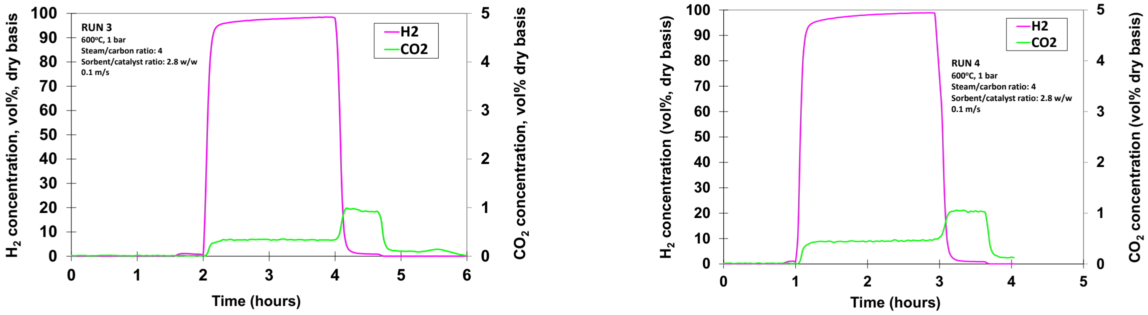

Fig. 8. SER consecutive tests in fluidized bed reactor with upgraded biogas as fuel ; Regeneration in nitrogen/steam added 2 vol% hydrogen.

5.2. Initial reforming and regeneration tests on the SER DBFB prototype

The results from the batch SER test run with upgraded biogas as fuel in the reformer reactor of the DBFB prototype are shown in Fig. 9. A stable high hydrogen production yield and a high CO_2 capture rate where also confirmed in this test, validating the proper functioning of the reformer with the chosen operating conditions. Temperatures at different levels of the bed were also quite homogeneous. Fluctuations of the steam flow are due to minor technical problems with the regulation system and the steam flow meter. In most of the test, the steam to carbon ratio was then between 3 and 4.

Results from the regeneration test following the SER test are shown in Fig. 10. The catalytic burner needs a minimum inlet air temperature to ignite. After several attempts, a good ignition was obtained for an air inlet temperature of 542 °C. Unfortunately, it was not possible to ignite the burner before this temperature was reached, and the middle temperature of the bed had already reached 750 °C, explaining why the calcination had already started. Nevertheless, after the electrical heating had been switched off and the burner took over, calcination continued to completion and the sorbent was fully regenerated. Unfortunately, a stable operation of the burner was obtained after the calcination was completed. However, it can be noticed that a linear and smooth temperature increase in the bed was registered when the burner operated in a stable regime. In this initial test, the burner was operated at 60% of its maximum power and it is expected that smoother operation should be achievable at 100%

power. It can also be noticed that the temperature measurements of the inlet manifold are not reflecting the real burner exhaust gas temperature. This is probably due to an unsuited positioning of the thermocouple which should have been placed at the entrance of a selected tube.

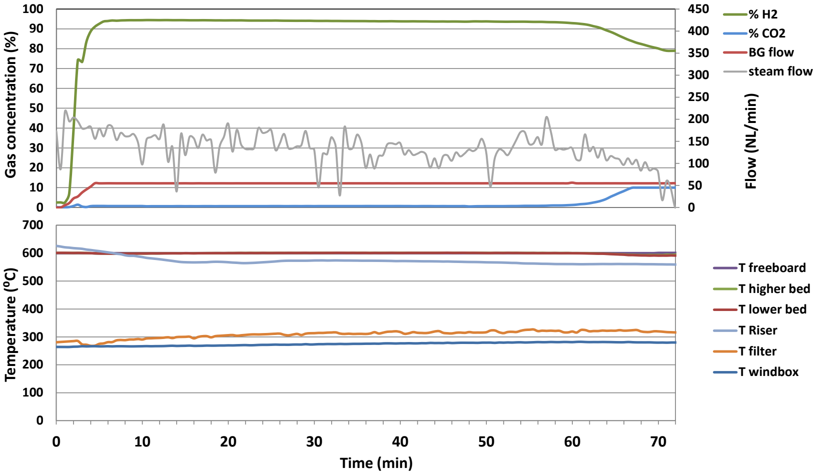

Fig. 9. SER batch test run with upgraded biogas as fuel in the DBFB reformer reactor.

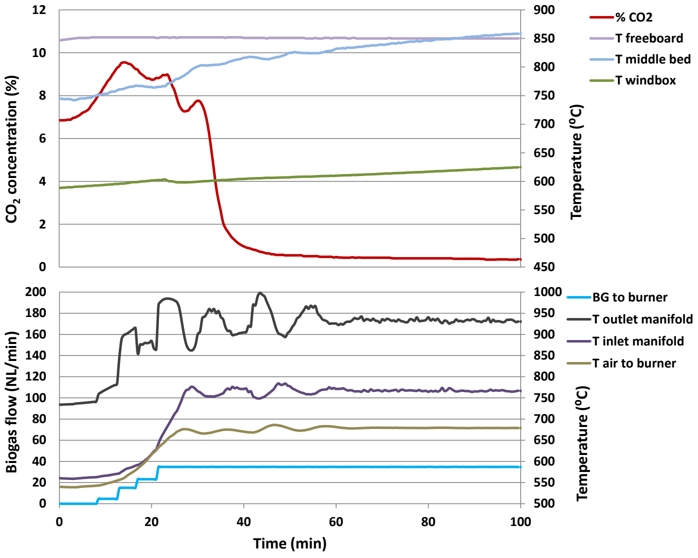

Fig. 10. Regeneration batch test using only the burner and the high temperature heat exchanger of the regenerator as heating source.

6. Conclusions and further work

In this paper, the design methodology and the technical specifications of a dual bubbling fluidized bed (DBFB) reactor prototype for sorption-enhanced reforming of upgraded biogas for hydrogen production has been presented. Reactor modelling and CFD calculations allowed detailed dimensioning of both the reactors and the high temperature heat exchanger of the regenerator. In addition, solids inventories, solids circulation rate and minimum required heat transfer from the regenerator's heat exchanger could be determined. Preliminary laboratory tests validated the pre-treatment method of the CO_2 sorbent, its sorption capacity, and carbonation kinetics. The addition of 2 vol% hydrogen in steam during the regeneration step proved an efficient protection of the nickel-based reforming catalyst against damageable oxidation-reduction cycles. Two initial batch tests run in the DBFB prototype proved the feasibility of operating the process. A high hydrogen concentration of 94 vol% and a high CO_2 capture rate were obtained while testing the reformer reactor. Full regeneration of the sorbent in batch mode was achieved using only the burner exhaust gas and the submerged heat exchanger as heating source, but further tests are required in order to tune and optimized this process step. Finally, the next phase of the work will involve the coupling of the solids loop between the reactors to test the process in a steady-state continuous mode.

Acknowledgements

This work is part of the BioSER project (Research Council of Norway, EnergiX Program, no. 216443). The authors would like to thank ZEG Power AS and the Research Council of Norway for financing the project and giving them the possibility to publish the work. Arnstein Norheim and Bjørg Andresen from ZEG Power are especially thanked for their valuable advices. HyNor Lillestrøm Renewable Hydrogen Test Center is also acknowledged for providing the necessary infrastructure to carry out this work.

Appendix A. Calculation of the overall heat transfer coefficient of the high temperature heat exchanger submerged in the regenerator

Equations that summarize the calculation of the convective and radiative heat transfer coefficients in the regenerator (tube to bed heat transfer) are listed below:

$$\frac{h_{c,tube-bed}\,l}{k_g} = \frac{0.125\varepsilon_{s,mf}}{B_1\left[1+B_2\left(\dfrac{k_g}{2C_{p_s}\mu_g}\right)\right]} + 0.165\,\mathrm{Pr}_g^{\frac{1}{3}}\left(\frac{\rho_g}{\rho_s-\rho_g}\right)^{\frac{1}{3}}\left(\frac{1}{B_3}\right) \qquad (9)$$

$$\varepsilon_{s,mf} = 1-\varepsilon_{mf} \qquad (10)$$

$$l = \left(\frac{\mu_g}{\rho_s-\rho_g}\right)^{\frac{2}{3}}\left(\frac{1}{g}\right)^{\frac{1}{3}} \qquad (11)$$

$$B_1 = 1+33.3\left[\left(\frac{U_e\rho_s C_{p_s}}{U_{mf}\,g k_g}\right)^{\frac{1}{3}} U_e\right]^{-1} \qquad (12)$$

$$B_2 = 1+0.28\varepsilon_{s,mf}^2.U_e U_{mf}\left(\frac{\rho_g}{\rho_s-\rho_g}\right)^{\frac{1}{2}}\left(\frac{\rho_s C_{p_s}}{g k_g}\right)^{\frac{2}{3}} \qquad (13)$$

$$B_3 = 1+0.05\left(\frac{U_{mf}}{U_e}\right) \qquad (14)$$

$$U_e = U_g - U_{mf} \qquad (15)$$

$$\mathrm{Pr}_g = \frac{C_{p_g}\mu_g}{k_g} \tag{16}$$

$$h_{r,tube-bed} = \frac{e_b e_{o-tube}}{e_{o-tube} + e_b - e_{o-tube} e_b} \cdot \frac{\sigma\left(T_{bed}^4 - T_{o-tube}^4\right)}{T_{bed} - T_{o-tube}} \tag{17}$$

$$A_{tube} = \frac{Q}{h_{tube-bed}\left(T_{o-tube} - T_{bed}\right)} \tag{18}$$

where k_g is the thermal heat conductivity of the gas in the regenerator, $\varepsilon_{s,mf}$ is the solids fraction in the bed at minimum fluidization velocity, ε_{mf} is the bed voidage at minimum fluidization velocity, ρ_s and ρ_g the densities of solids and gas in the regenerator respectively, Cp_g is the gas mass heat capacity in the regenerator, Cp_s is the solids mass heat capacity, μ_g is the gas viscosity in the regenerator, g is the gravitational acceleration, Pr_g is the Prandtl number, U_g is the fluidization gas velocity in the regenerator, U_e the excess gas velocity above the minimum fluidization velocity U_{mf}, σ the Stefan-Boltzman constant, T_{bed} is the particle bed temperature in the regenerator, T_{o-tube} is the outer tube temperature of the heat exchanger, A_{tube} is the total immersed surface area of the heat exchanger, Q the minimum required heat to be transferred to the regenerator, and $h_{tube-bed}$ the overall heat transfer coefficient.

References

[1] Fuel Cells and Hydrogen Joint Undertaking, Programme Review 2012. ISBN 978-92-79-29158-6

[2] European Hydrogen Association. http://www.h2euro.org/wp-content/uploads/2013/04/press-release-Hydrogen-refuelling-stations-worldwide.pdf

[3] Mohseni F, Magnusson M, Görling M, Alvfors P. Biogas from renewable electricity – Increasing a climate neutral fuel supply. Applied Energy, 90, 2012, p. 11-16

[4] Ulleberg Ø, Meyer J, Eriksen J, Norheim A, Gjerløw JC. Hynor Lillestrøm – A renewable hydrogen station & technology test center. 20th World Hydrogen Energy Conference 2014, Gwangju, Korea.

[5] Harrison DP. Calcium enhanced hydrogen production with CO_2 capture. Energy Procedia, Vol. 1, Issue 1, 2009, p. 675-681

[6] Lopez Ortiz A, Harrison DP. Hydrogen production using sorption-enhanced reaction. Ind. Eng. Chem. Res., 40, 2001, p.5102-5109

[7] Johnsen K, Ryu HJ, Grace JR, Lim CJ. Sorption-enhanced steam reforming of methane in a fluidized bed reactor with dolomite as CO_2-acceptor. Chemical Engineering Science, 61, 2006, p. 1195-1202

[8] Abanades JC, Alvarez D. Conversion limits in the reaction of CO_2 with lime. Energy & Fuels, 17, 2003, p. 308-315

[9] Mastin J, Aranda A, Meyer J. New synthesis method for CaO-based synthetic sorbents with enhanced properties for high temperature CO_2-capture, Energy Procedia, Vol. 4, 2011, 1184-1191

[10] Lindborg H, Jakobsen HA. Sorption enhanced steam methane reforming process performance and bubbling fluidized bed reactor design analysis by use of a two-fluid model. Industrial Engineering Chemistry Research, 48(3), 2009, p. 1332-1342,

[11] Stendardo S, Foscolo PU. Carbon dioxide capture with dolomite: A model for gas-solid reaction within grains of a particulate sorbent. Chemical Engineering Science, 64, 2009, 2343-2352

[12] Johnsen K, Grace JR, Elnashaie SSEH, Kolbeinsen L, Eriksen D. Modeling of sorption-enhanced reforming in a dual bubbling bed reactor. Industrial Engineering Chemistry Research, 45, 2006, p. 4133-4144

[13] Lee DK, Baek IH, Yoon WL. Modeling and simulation for the methane steam reforming enhanced by in-situ removal utilizing the CaO carbonation for H_2 production. Chem. Eng. Sci., 59(4), 2004, p. 931-942

[14] Wang Y, Chao Z, Jakobsen HA. 3D simulation of bubbling fluidized bed reactors for sorption enhanced steam methane reforming processes. Journal of Natural Gas Science and Engineering, 2, 2010, p. 105-113

[15] Orcutt JC, Davidson JF, Pigford RL. Reaction time distributions in fluidized catalytic reactors. Chemical Engineering Progress Symposium Series, 58(38), 1962, p. 1-15

[16] Johnsen K. Sorption-enhanced steam methane reforming in fluidized bed reactors. Doctoral Thesis at NTNU, 2006:116

[17] Xu J, Froment GF. Methane steam reforming, methanation and water gas shift- I. intrinsic kinetics. AIChE Journal, 35, 1989, p. 88-96

[18] Handbook of fluidization and fluid-particle systems. Yang WC. ISBN 0-8247-0259-X

[19] Molerus O, Burschka A, Dietz S. Particle migration at solid surfaces and heat transfer in bubbling fluidized beds II – Prediction of heat transfer in bubbling fluidized beds. Chem. Eng. Sci., 50, no. 5, 1995, p. 879-885

[20] Ozkaynak TF, Chen JC, Frankenfield TR. An experimental investigation of radiant heat transfer in high temperature fluidized bed. Fluidization IV. New York, Engineering Foundation, 1983, p. 371-378